

# Design and Characterization of a Plug-in Device for Tactile Sensing

Go Otsuka, Masato Niwa, Toshio Kawanishi and Goro Obinata

*Department of Robotic Science and Technology, Chubu University, Kasugi 487-8501, Japan*

**Keywords:** Tactile Sensor, Vision-based, Plug-in System, Mechanical Quantity, Adhesiveness.

**Abstract:** Although the most of the functions of the human upper body can be performed by robotic technologies which are already developed, the hand and finger functions cannot be achieved by artificial alternatives, particularly concerning the dexterous manipulation. One of the reasons is the lack of tactile sensors like the ones observed in the human fingertip. The purpose of this paper is to design a vision-based tactile sensor with the size of a fingertip, and evaluated it under several conditions of contact. The resolution performance of the developed vision-based sensor for measuring contact force and contact moment is shown based on preliminary experiments. Moreover, the results of these experiments show the potential of the proposed sensor for evaluating adhesive surfaces.

## 1 INTRODUCTION

In industry, there is a demand to replace the work of human resources by autonomous systems. Although the most of the functions of the human upper body can be performed by already developed robotic technologies, the hand and finger functionalities cannot be achieved by artificial alternatives, particularly concerning the dexterous manipulation. One of the reasons is the lack of tactile sensors like the ones observed in the human fingertip. Different types of tactile sensors have been proposed for several purposes (Shinoda, 2002; Lee and Nicholls, 1999; Maeno, et al., 1998). However, there are a few artificial fingertip sensors with the sensibility high as the human's fingertips. It is challenging for artificial finger tips to obtain multi model tactile sensation with small volume and soft surface of contact. This happens because the difficulty on installing several single-purpose sensors in a fingertip-sized chassis, or from the mechanical requirements of covering the surface of sensor with soft material. In order to solve this problem, the MEMS-based sensors can be made compact in size (Wen and Fang, 2008), but the sensitivity decreases when the surface is covered with elastic material. The problem has been improved for obtaining high sensitivity in temporal and space resolution by several ideas (Jamone et al., 2015; Shin et al., 2018). However, there is still the problem of the multi-modal haptic sensing with single sensor.

Vision-based sensors with soft surface were proposed to achieve tactile sensation like the ones observed in human fingertips (Obinata, et al., 2007; Ito, et al., 2011a; Ito, et al., 2011b; Ito, et al., 2012; Ito, et al., 2014). Its design consists of a digital camera, LED light and a soft-pad for touching. The measurement is based on deformations of the pad surface, which reflects the contact surface. A very small camera captures the alterations in the pad surface, and an algorithm is able to analyze the changes in the images in order to measure the contact surface. The sensor is able to measure dynamic characteristics: multi-dimensional force and moment, degree of adhesion and shape of the contact surface. The important feature worth noting is that the sensor is able to estimate the adhesion degree with the contact surface, then determine whether the contact object moves (macro slipping) or stays with the sensor surface (incipient slip) under a certain amplitude of pressure force. This means that the sensor is able to provide information in order to prevent from macro slipping based on the estimating degree of adhesion with the contact surface (Ito, et al., 2011a). This type of sensor has been designed to the medical use of palpation for pathological soft tissues because the sensor could be integrated with the endoscope (Yeh et al., 2010).

Although vision-based sensors have various advantages, such as the ability of estimating adhesion degree, these sensors still did not reached the high implementability performance. One of the main

reason is the usage of analog cameras and the signal converters used, which require dedicated hardware and software resources (Ito, et al., 2014). This situation has changed nowadays due to the usage of digital cameras and its accessible firmware. Also, the size and cost reduction of digital cameras, has potentially raised the application which uses digital cameras on robotic applications.

The purpose of this paper is to design a vision-based tactile sensor with the size of fingertip using small digital cameras which have been recently available with low cost, and to characterize it under several conditions of contact. This paper is described as follows: The structure and the components are illustrated in chapter 2. Chapter 3 describes the developed software to read the obtained image. The preliminary results of the experiments, which shows the resolution of the sensor for measuring contact force and contact moment, are given in chapter 4. Then in chapter 5, it is described experiments with compliant objects having adhesive surfaces. Finally, the chapter 6 show the conclusion and future works

## 2 STRUCTURE OF SENSOR

The designed vision based tactile sensor consists of a CMOS camera, a touch pad, a half mirror and a surface-emitted LED. The components are shown with the placements in Figure.1. The values are  $L = 12\text{mm}$ ,  $B = 7\text{mm}$ ,  $W = 27\text{mm}$ ,  $H = 20\text{mm}$ , and  $D = 19\text{mm}$ . The CMOS camera works with preinstalled lens. The angular field of view of the lens is 53 degrees, and the focal length is 19mm. The size of the sensor is defined according to these values. The pad is transparent and soft, and it is installed to the casing with a transparent rigid liner.

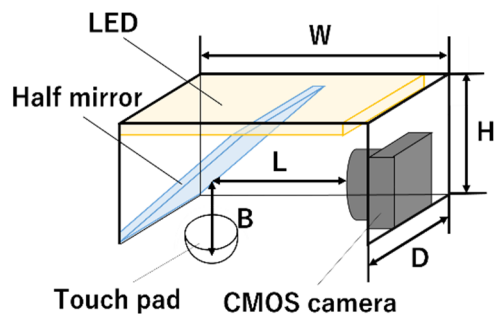


Figure 1: Structure and dimensions of the sensor.

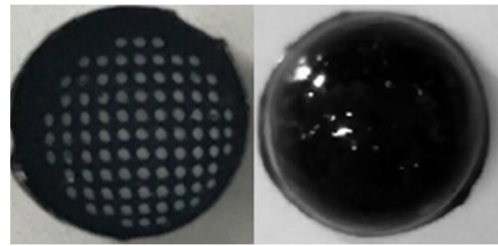


Figure 2: Touch pad.

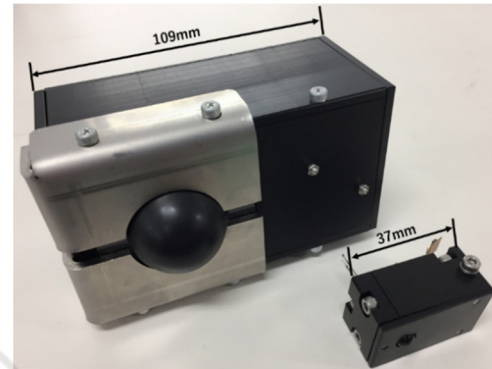


Figure 3: Examples of different sizes for the developed sensor.

The rigid liner is set to prevent the pad from being moved inward the sensor structure. The CMOS camera captures the inside image of the touch pad through the half mirror. A picture of the touch pad is shown in Figure 2. A black rubber membrane covers the pad surface. White dots are printed into a lattice pattern inside of the membrane, with pitches of  $0.1\text{mm}$ , on both directions. Through the dots position, it is possible to calculate the deformation of the pad. The details about the method of analyzing the deformation of the touch pad to estimate the targets are described in the following chapters. The structure of the entire sensor has only 4 components, allowing large freedom in scalability of sensor design as show in Figure 3, where the sensor can have different sizes.

## 3 SPECIFICATION AND SOFTWARE

In this chapter it is described the details regarding the software used to analyze the image from the touch pad, and specification regarding the implementation of the components present in the sensor structure. Table 1 and Table 2 show the specification of COMS camera and the USB interface to PC.

Table 1: CMOS camera (Asahi Electro. Lab., PPV404C).

External dimensions	8.0mm×8.0mm×5.5mm
Image pickup device	1/4 inch CMOS Color image sensor
Digital output compatible	YUV422/RGB565 8bit Parallel output
Pixel size	5.55μm×5.55μm
Angle of view	51°
Focal length	19mm
Number of pixels	640(H) ×480(V)
Frame cycle	MAX30fps

Table 2: USB interface (AEL-USB-A).

External dimensions	20mm×45mm×7.3mm
Input voltage	USB bus power
External connection method	USB-mini B
Operation guarantee temperature	0℃~70℃

The USB interface makes it possible for the sensor to transmit the captured images to a desktop computer. There is no particular requirement for that communication, since the USB interface in the operational system handle the process. It was developed a program which translates the deformation of the pad to desired contact information. The program (written in C++) includes *openCV* functions for the image processing.

Depending on the application, it should be selected the appropriate configuration for the digital camera, which relies on two main aspects: the communication frame rate and the camera resolution. The image acquisition frame rate of the touch pad is highly related to the required sampling rate of the control loop, if the sensor is applied for robot gripper control. If the control loop requires a reference parameter with a higher rate, then the communication speed need to be higher as possible.

Nowadays digital cameras are available with high communication speed. However, higher resolution of measuring physical quantity, like multi-dimensional force, requires the higher space resolution of the camera. Such higher resolution means much image information, and results in more computational time. This means that there is a trade-off between the measuring resolution and the speed of processing.

#### 4 EXPERIMENTAL RESULTS OF FORCE MEASUREMENT

In order to show the potential of the designed sensor, experiments of force sensing were carried out. It was

assumed that the contact object for the sensor has flat surface. The idea for measuring the force and moment at the sensor pad is to observe the relation between the amount of characteristics in the captured image from the pad and the physical quantities, such as force and moment.

##### 4.1 Normal Force

When a normal force is applied to the sensor pad with a flat surface, the dots on the captured image move radially from the center to the outside of the pad. This movement is quantified according to the default distance between the dots in the touch pad to the distance presenting in the image. The distance between two dots located at each opposing corner, as show in Figure 4, is taken for the quantification.

The two distances are measured, and its average value is calculated. In Figure 5, the average values are compared with the applied normal forces, which are measured by a calibrated equipment (3 dimensional force sensor: USL06-H5200N-C, Tec Gihan). There is a linear direct relationship between the applied normal force and the distance on the captured image. This makes it possible to estimate the normal force from the image of the pad.

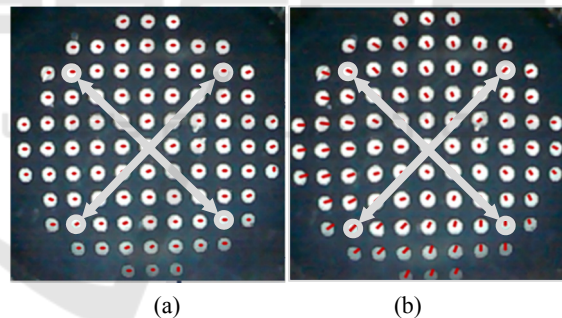


Figure 4: Definition of the distances. (a) Image in non-contact state. (b) Image under a normal force.

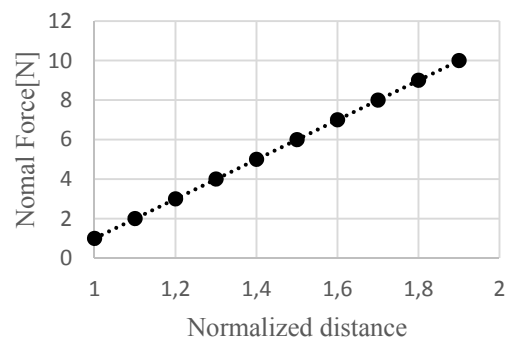


Figure 5: The normal force and the average of the two normalized distances.

### 4.2 Tangential Force

The dots on the captured image move to the opposite direction when a tangential force is applied to the sensor pad flat surface. This movement is quantified according to the dots displacements on the image. We take the displacements of nine dots around the center of the touch pad (see the red circles in Figure 6). It is measured the displacements of these dots, and the average value is calculated. In Figure 7, the average values are compared with the applied tangential forces, which are measured by the same equipment as normal force calibration. The relationship between the tangential force applied to the dots deformation is show in the Figure 7. From this information it is possible to estimate the tangential force applied to the touch pad surface.

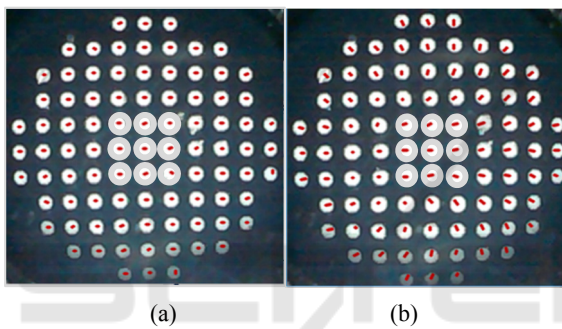


Figure 6: Definition of the nine dots and the displacements. (a) Image in non-contact state. (b) Image under a tangential force.

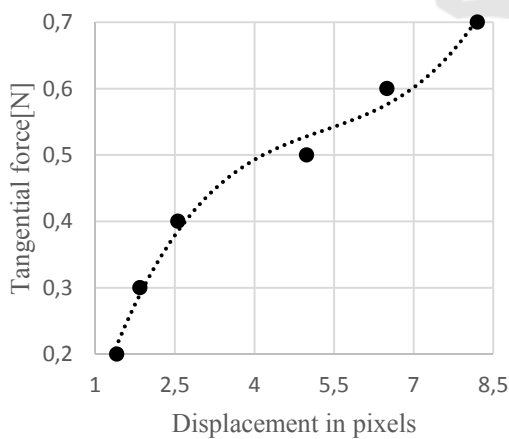


Figure 7: The relation between the tangential force and the average value of the nine dots displacements.

### 4.3 Moment

When a certain amount of rotational moment is applied to the sensor pad flat surface, some dots around the center on the captured image do a rotational movement in the opposite rotational direction to the moment applied. The rotation is quantified following the same procedure used for the tangential and normal forces. The calculation focus on the four dots around the center dot, and it is calculated the rotation angle based on the touch pad when no rotational force is applied (see the red circles in Figure 8). It is measured the rotation angles from the four dots locations. In Figure 9, the values are compared with the applied moments, which are measured by a calibrated device for moment value. The estimation of the moment is calculated in the same way as the tangential and normal force.

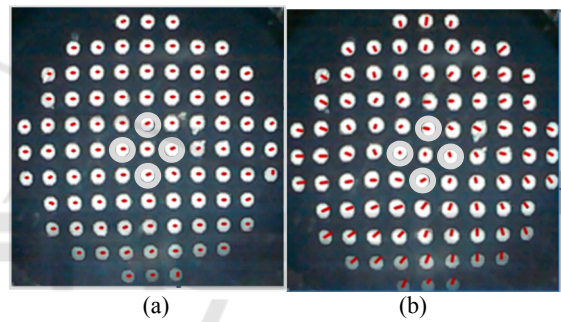


Figure 8: Definition of distances. (a) Image in non-contact state. (b) Image under a moment.

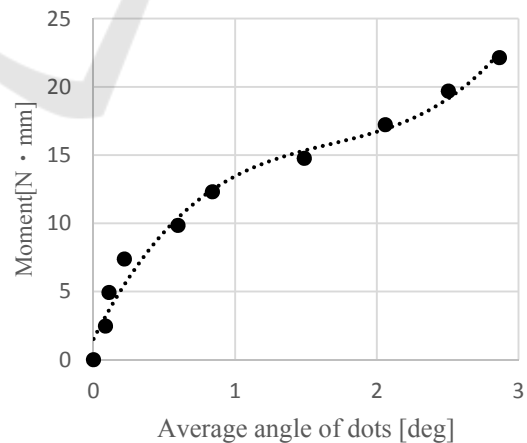


Figure 9: The relation between moment and the rotation angle.

## 5 SENSING WITH ADHESIVE SURFACE

One of the feature present in the developed sensor is the ability to measure contact area of interaction. It is possible to apply the sensor observation to analyze the slide processes from adhesive objects.

This indicates the possibility for evaluating adherence property. To confirm this possibility, series of experiments were conducted where the sensor touched an adhesive surface with a certain amount of pressure and peeled off.

It is measured the change in the different types of forces during the sliding process. Figure 10 shows an example of the time response in the normal force acting between the sensor pad and the object surface. The temporal sequence of the contact area is also shown in the figure. First, the initial force with predefined amplitude was applied to the object surface with the touch pad of sensor, and then started a process to lower the force from time T1. The force reached the minimum at time T2. It is noted that the pressure at T2 took negative value and it relaxed afterwards. The final value of the contact area did not become zero, even if the force became zero. This happens because the estimation algorithm of the sensor for measuring the contact area has a certain error. The algorithm is based on distinguishing the border of the contact area and the non-contact area on the captured image. Improvement on this approach will be required to obtain better estimates.

Two different objects were selected to measure the force and the contact area during experiments of attaching/peeling-off. Those objects are different both in the elastic compliance and in the adhesiveness. The behaviour of the peeling-off process can be illustrated in force-area space; one example of force-area plot is given in Figure 11. The peeling-off process starts at Pb and the point indicated by the pair of forces and contact area moves towards the left lower region along the dotted line and reaches Pe. To characterize the adherence property, five parameters are defined in the force-area space, and the notations are given in Table 3. The other parameters defined below are normalized ones for evaluation over different materials of touching objects.

The  $So/Sb$  is the normalized residual area, and  $Se/Sb$  is the normalized area at the maximum tensional force. The  $-Fp/Fi$  is the normalized force amplitude which is required for starting peeling-off.

The experimental results with two objects are shown in Table 4 and Table 5. Table 4 summarizes the result for the surface of absorption in gel

(polyurethane, Cram Works), which is a material used to isolate vibrations waves.

The force for peeling  $-Fp$  increased according to the initial applied force  $Fi$ . The normalized values  $-Fp/Fi$  took a certain value bigger than 1 and decreased to 1 as the initial force increased. The residual area is

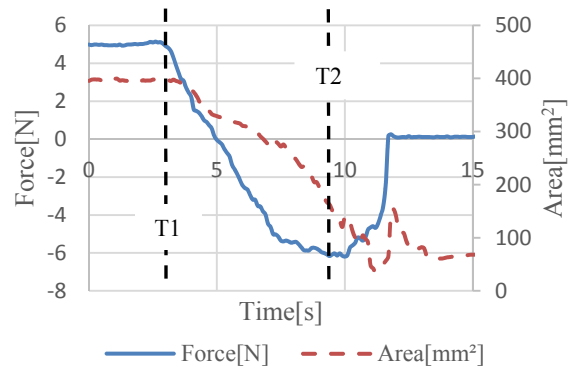


Figure 10: The time responses in force and contact area.

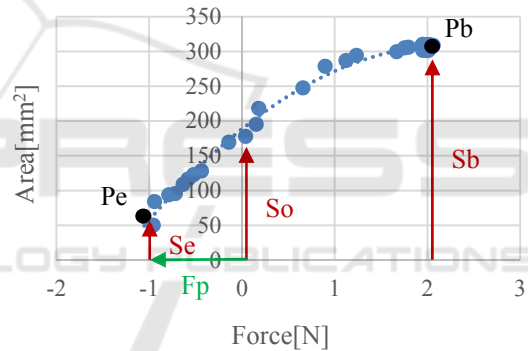


Figure 11: Force-area space of sliding.

Table 3: Notations on sliding process.

$Fi$ [N]	Initial applied force
$Sb$ [mm <sup>2</sup> ]	Initial contact area
$So$ [mm <sup>2</sup> ]	Contact area when the applied force becomes zero (Residual area)
$Se$ [mm <sup>2</sup> ]	Contact area at the maximum tension with the adhesive surface and the sensor surface
$Fp$ [N]	Force for tearing-off (Adhesive strength just before tearing off).

Table 4: Parameters for adhesiveness (surface:adsorbing gel, body:polyurethane).

$Fi$ [N]	$Sb$ [mm <sup>2</sup> ]	$So$ [mm <sup>2</sup> ]	$Se$ [mm <sup>2</sup> ]	$Fp$ [N]	$So$ /Sb	$-Fp$ /Fi
1	240	200	80	-3.7	0.83	3.7
2	240	215	90	-4.6	0.9	2.3
3	350	275	100	-4.3	0.79	1.43
4	380	320	100	-4.3	0.84	1.075
5	400	350	130	-5.5	0.88	1.1

Table 5: Parameters for adhesiveness. (surface: polyethylene and inorganic mineral filler, body: synthetic rubber).

Fi [N]	Sb [mm <sup>2</sup> ]	So [mm <sup>2</sup> ]	Se [mm <sup>2</sup> ]	Fp [N]	So/ Sb	-Fp /Fi
1	190	155	150	-0.25	0.82	0.25
2	300	175	100	-0.4	0.58	0.2
3	430	220	100	-0.4	0.51	0.133
4	400	220	100	-0.4	0.55	0.1
5	450	225	100	-0.45	0.5	0.09

then increased according to the initial applied force  $F_i$ ; However, the normalized values  $So/Sb$  showed approximately constant values without depending on the initial force  $F_i$ . The normalized residual area  $So/Sb$  showed the values over 0.8 and there was no large variation. From the results, it is observed a certain amplitude of force is required to peel off; however, larger forces are required to peel off when larger initial forces are applied. It is also observed that there is a contact area which is independent on the initial force.

The results of another adhesive object: polyethylene and inorganic mineral filler (synthetic rubber, Kokuyo) are summarized in Table 5. The force for peeling-off  $-F_p$  kept constant except for the case of weakest initial force. The normalized residual area showed small values in comparison with the former surface. The normalized residual area  $So/Sb$  decreased when the initial force increased, and the values are smaller in comparison with the former object. The tendencies of the parameters in those two adhesive surfaces are different; therefore, the parameters may characterize the adhesiveness.

These experimental results suggest the possibility for evaluating adhesive surfaces. There exist problems for generalizing the parameters; for an example, the parameter values are dependent on the radius of the touch pad of the sensor. Moreover, the results may depend on the stiffness properties of the sensor pad and the object on contact.

## 6 CONCLUSIONS

This paper shows the design of a vision-based tactile sensor with the size of fingertip. All the components found in the mechanical design are accessible for the present market. The main component is a digital camera, and the data communication interface can be found in most of PC operational system. The software is designed to be used widely by other modules (by a control module for example). The preliminary experimental results show the resolution performance of the sensor for measuring contact force and contact

moment. The paper also describes the experiments with compliant objects having adhesive surfaces. From these experiments, parameters for evaluating adhesive surfaces have been proposed. The results on the parameters show the potential of this sensor for evaluating adhesiveness.

The design variation will be required for the specific applications of the medical devices, haptic feedback systems, human interfaces, and so on. The less number of components of this sensor will make it easy to develop for such applications. More precious arrangement and estimation method for measuring contact area are expected to adhesive evaluation with this type of sensor.

## ACKNOWLEDGEMENTS

The authors would like to thank BYNAS Co., Ltd, OOTAHIRO Co., Ltd, ITOBIGEISHA-SEIHAN-SHO Co., Ltd for their helps in production of the sensor.

The authors would like to thank Nicholas de Bastos Melo for his kindly improving English expressions in the manuscript.

## REFERENCES

- Ito, Y., Kim, Y., and Obinata, G. (2011a). *IEEE Sensors Journal*, 11(9):2037-2047.
- Ito, Y., Kim, Y., Nagai, C., and Obinata, G. (2011b). *Int. J. Adv. Robot. Syst*, 8(4):25-234.
- Ito, Y., Kim, Y., Nagai, C., and Obinata, G. (2012). *IEEE Trans. Autom. Sci. Eng*, 9(4):734-744.
- Ito, Y., Kim, Y., and Obinata, G. (2014). *Adv. Robot. Autom*, 3(1):1-9.
- Jamone L., Natale L., Metta, G., Sandini G. (2015). *IEEE Sensors Journal*, 15(8):4226-4233.
- Lee, M. H. and Nicholls, H. R. (1999). *Mechatronics*, 9:1-31.
- Maeno, T., Kobayashi, K., Kawai, T., and Hirano, Y. (1998). *Japanese Society of Mechanical Engineers*, 64(620): 1258-1265.
- Obinata, G., Ashish, D., Watanabe, N., and Moriyama, N. (2007). *Mobile Robots: Perception & Navigation*, pro literature Verlag, Mammendorf, Germany: 137-148.
- Shin, K., Sim, M., Park, H., Cho, Y., Sohn, J. I., Cha, S. N., Jang, J. E. (2018). *Proceedings of Haptic Symposium, San Francisco*: 95-99.
- Shinoda, H. (2002). *Japanese Robotic Society*, 20(4):385-388.
- Wen, C. and Fang, W. (2008). *Sensors and Actuators A: Physical*, 145-146:14-22.
- Yeh, C. S., Ju, M. S., Martynenko, Y., Goryacheva, I. Su, F. C. (2010), *6<sup>th</sup> World Congress of Biomechanics, Singapore, IFMBE Proceedings*, 31:1270-1273.